Synthetic and Systems Biotechnology 9 (2024) 406–415

Contents lists available at ScienceDirect

Synthetic and Systems Biotechnology

journal homepage: www.keaipublishing.com/en/journals/synthetic-and-systems-biotechnology

Original Research Article

Design and engineering of logic genetic-enzymatic gates based on the activity of the human CYP2C9 enzyme in permeabilized *Saccharomyces cerevisiae* cells

Rana Azeem Ashraf, Matthias Bureik, Mario Andrea Marchisio *

School of Pharmaceutical Science and Technology, Tianjin University, 300072, Tianjin, China

ARTICLE INFO

Keywords:
Cytochrome P450
Drug metabolism
Budding yeast
Diclofenac
Synthetic biology
CORM-401
Boolean gates

ABSTRACT

Gene circuits allow cells to carry out complex functions such as the precise regulation of biological metabolic processes. In this study, we combined, in the yeast *S. cerevisiae*, genetic regulatory elements with the enzymatic reactions of the human CYP2C9 and its redox partner CPR on luciferin substrates and diclofenac. *S. cerevisiae* cells were permeabilized and used as enzyme bags in order to host these metabolic reactions. We engineered three different (genetic)-enzymatic basic Boolean gates (YES, NOT, and N-IMPLY). In the YES and N-IMPLY gates, human CYP2C9 was expressed under the galactose-inducible *GAL1* promoter. The carbon monoxide releasing molecule CORM-401 was used as an input in the NOT and N-IMPLY gates to impair CYP2C9 activity through inhibition of the Fe^{+2}- heme prosthetic group in the active site of the human enzyme. Our study provides a new approach in designing synthetic bio-circuits and optimizing experimental conditions to favor the heterologous expression of human drug metabolic enzymes over their endogenous counterparts. This new approach will help study precise metabolic attributes of human P450s.

1. Introduction

Despite various morphological and cellular differences maturated over a billion years of separate evolution, humans and yeasts share several genetic resemblances [1]. Over the last few years, synthetic biology has contributed to establish humanized yeasts as important tools to study functional expression and characterization of human genes [2]. This was achieved through genetic manipulations, which did not affect the building blocks of life, of *Saccharomyces cerevisiae* and *Schizosaccharomyces pombe* cells that have become the chassis for circuits hosting human genes [3]. Both yeast species have played vital roles in elucidating complex biological processes of human biology and diseases such as cancer [4]. Moreover, *S. pombe* and *S. cerevisiae* are widely used for the expression of drug metabolic enzymes (DMEs) [5].

By leveraging our deep understanding of yeast biology and genetic resources, we have previously implemented a wide variety of biological circuits, especially biosensors, that were based on transcription/translation regulatory mechanisms in budding yeast [6]. The yeast *S. cerevisiae* represents a commonly used chassis for synthetic gene circuits because it is a unicellular eukaryotic organism whose genome is well annotated and relatively easy to manipulate by using homologous recombination [7]. Synthetic gene digital (logic) circuits have become the subject of many studies due to their various possible applications, such as diagnostics, environmental care, and DNA computing [8]. In digital circuits, the inputs and the output take only two values: 0 (small concentration of input small molecules; low output signal, e.g., fluorescence) and 1 (large concentration, high signal). Logic behavior is reproduced by the action of regulatory factors and chemicals on the promoters and the mRNA of biological Boolean gates [9,10]. Inputs for genetic circuits are chemicals that are divided into two classes depending on their action on transcription and translation: inducers and corepressors [11]. Inducers favor protein synthesis since they either inactivate repressors or activate activators. Corepressors, in contrast, prevent protein production because they activate repressors or inactivate activators. A reporter protein acts as a single output.

Many human cytochrome P450 enzymes (CYPs or P450s) are expressed in the liver, where they carry out the metabolism of xenobiotics and endobiotics by converting them into inactive substances that are excreted from the body via urine or bile. Thus, P450s are important for maintaining homeostasis and metabolising drugs [12]. Human

Peer review under responsibility of KeAi Communications Co., Ltd.
* Corresponding author.
E-mail addresses: azeem_rana@yahoo.com (R.A. Ashraf), matthias@tju.edu.cn (M. Bureik), mamarchisio@yahoo.com, mario@tju.edu.cn (M.A. Marchisio).

https://doi.org/10.1016/j.synbio.2024.03.013
Received 27 January 2024; Received in revised form 10 March 2024; Accepted 17 March 2024
Available online 29 March 2024

cytochrome P450s have been expressed in *S. pombe* for long time [13–18]. In particular, the permeabilized fission yeast system known as *enzyme bags* is a very efficient platform to scrutinize all human P450s against any potential candidate drug in a quick time [13,19].

After successfully establishing the Triton X-100-permeabilization-based enzyme bags in *S. pombe* (and applying it to recombinant strains expressing human P450s [19]), we set-up a similar Triton X-100-permeabilized system in *S. cerevisiae*.

A DNA sequence encoding for the 2A peptide from the equine rhinitis B virus-1 (EBRV-1) was used to construct two synthetic *S. cerevisiae* bicistronic transcription units (TUs) where either the human *CPR* or *CYP2C9* gene was linked to the yeast enhanced green fluorescence protein (*yEGFP*) [20,21]. Strains successfully transformed with the two TUs were characterized via fluorescence measurements and then permeabilized using 0.3 % concentration of Triton X-100. The functionality of the CPR-CYP2C9 system in *S. cerevisiae* enzyme bag was proven on two different kinds of substrates: diclofenac, whose metabolites were detected via by LC-MS-MS (liquid chromatography with tandem mass spectrometry), and proluciferin substrates that led to the emission of bioluminescent signals.

By means of *S. cerevisiae* enzyme bags, we managed to design and engineer basic Boolean gates—such as NOT, YES, and N-IMPLY—in a novel way that exploits metabolic reactions—involving human CYP2C9—either alone or together with the control of gene expression. The former were referred to as enzymatic Boolean gates, the latter as genetic-enzymatic ones. In a genetic-enzymatic YES gate, CYP2C9 was expressed under the inducible *GAL1* promoter (pGAL1), whereas in the enzymatic NOT gate, CYP2C9 was constitutively expressed but its activity was inhibited by CORM-401 (a carbon monoxide releasing molecule) [22] since CO binds to the central iron in the prosthetic heme group of CYP enzymes and impairs their function. The combination of these two gates led to the construction of a two-input genetic-enzymatic N-IMPLY gate that delivers, as an output, the product of CYP2C9-driven metabolism only in the presence of galactose and the absence of CORM-401.

2. Materials and Methods

2.1. Materials and growth media

All chemicals used in this study are of analytical grades 99–100%. Most of them were bought from Sigma-Aldrich Chemical (Schnelldorf, Germany), while other reagents were procured from reliable commercial sources in China. Bacterial competent cells (*E. coli* DH5α, Life Technology-18263–012) were grown in Luria Bertani (LB) plates containing: bacto-tryptone 10 g/L, yeast extract 5 g/L, NaCl 10 g/L, and agar 15 g/L. Yeast transformation was done using the lithium-acetate protocol [23] that demands to use polyethylene glycol (PEG) solution, 10% dimethyl sulfoxide (DMSO), salmon sperm DNA (ssDNA) solution (Sigma-Aldrich, product number 16–201), and lithium acetate mixture. Tris-HCl was bought from AKZ-Biotech (Tianjin, China), Triton X-100 from Leagene (Beijing, China), white 96-well microtiter plates from Nunc (Thermo-fisher scientific, Lagenselbold, Germany). The NADPH regeneration system, luciferin H (probe for CYP2C9), and light detection reagent (LDR) came from Promega (Madison, USA). CORM-401 carbonyl[N-(dithiocarboxy-κS,κS')-N-methylglycine]manga-nite and diclofenac were purchased from Sigma-Aldrich (Deisenhofen, Germany). Diclofenac was dissolved in pure methanol as a 10 mM stock solution. CORM-401 was dissolved in DMSO and aliquots were stored at −20 °C. The compound is stable under these conditions and releases CO (2–3 mol CO per mol CORM-401) only in the presence of CO acceptors such as heme proteins [24,25]. CORM-401 stock solution was heated at 37 °C just before adding it to a reaction mixture with substrates and it was always protected from light. Luc-BE, Luc-2FBE, Luc-3FBE, Luc-CEE, Luc-FEE, Luc-EE, Luc-FuBE, Luc-PE, and Luc-CPE were synthesized by our collaborative group [17,26–28]. All other chemicals and reagents used in this work are of the highest available grade. SDC (synthetic defined complete medium) with 2% glucose or 2% galactose was used for the growth of yeast cells expressing TUs under pGPD only or pGPD/pGAL1 for 18 or 30 h respectively.

2.2. Plasmid construction

All integrative plasmids constructed in this work (a complete list and description is given in Table S1) are based on the pRSII40X yeast shuttle vector collection [29] (available at Addgene-35442, a gift from Steven Haase). Touchdown PCR with Q5 High-Fidelity DNA Polymerase (NEB-M0491S) was employed to extract DNA sequences from their original plasmids. PCR products were eluted from agarose gel using the AxyPrep DNA extraction kit (Axigen, AP-GX-250). The pRSII40X vectors were cut-open with *Acc*65I (NEB-R0599S) and *Sac*I (NEB-R3156S). DNA parts and cut-open backbone were linked together via the isothermal assembly method [30]. *E. coli* competent cells were transformed with our plasmids (30 s heat shock at 42 °C) and grown overnight at 37 °C in LB broth or plates supplied with ampicillin (0.1 mg/mL). Plasmid extraction from bacterial cells was carried out by using standard methods [31]. All plasmids were sequenced via Sanger method to check the correctness of the inserts. The sequences of all parts used in this work are given in Table S2.

2.3. Yeast strain construction

Each of our new plasmids was placed into the genome of the *S. cerevisiae* strain byMM584, i.e., CEN.PK2–1C (MATa; his3D1; leu2-3_112; ura3−52; trp1−289; MAL2-8c; SUC2), Euroscarf-30000A (Johann Wolfgang Goethe University, Frankfurt am Main, Germany). Yeast transformation was performed as described [23]. Plasmids (about 5 μg) were linearized at the corresponding auxotrophic marker with a proper restriction enzyme. Transformed cells were grown for about 48 h at 30 °C on plates (glucose 2%, agar 2%) containing a synthetic selective medium. All synthetic yeast strains realized in this work are listed in Table S3.

2.4. Flow cytometry

Yeast cells containing the bi-cistronic sequences "hCPR-ERBV-1 2A-yEGFP" and "hCYP2C9-ERBV-1 2A-yEGFP" under pGPD were initially grown for 18 h in SDC supplied with 2% glucose at 30 °C and 240 RPM. Then, cell cultures were 1:100 diluted in SDC before fluorescence measurements. Yeast cells containing the bi-cistronic sequences "hCPR-ERBV-1 2A-yEGFP" under pGPD and "hCYP2C9-ERBV-1 2A-yEGFP" under pGAL1 were grown, first, for 30 h in SDC (supplied with 2% glucose) at 30 °C and 240 RPM. Then, these cell cultures were 1:100 diluted (and induced) in SDC supplemented with 2% galactose. Cells grew for about 28 h at 30 °C and 240 RPM before fluorescence measurements. Green fluorescence was measured using a BD FACSVerse Flow Cytometer (blue laser 488 nm and emission filter 527/32 nm). The FACS (fluorescence activated cell sorting) machine setup was checked at the beginning and end of each experiment using fluorescent beads (BD FACSuite CS&T Research Beads 650621). Measurements were considered as reliable only when the relative difference between the initial and final values of the peaks of the beads was not higher than 5%. Each strain was measured at least in three independent experiments (i.e., the cells were cultured on different days). Thirty-thousand events were collected during each experiment. Data were analyzed using the flowcore R-Bioconductor package [32]. The background fluorescence, i.e., the fluorescence associated with the strain byMM584 (the chassis of our circuits that did not contain any fluorescence source) was subtracted from the mean fluorescence value of each engineered strain. Standard deviations were calculated on these mean values.

2.5. Biotransformation with enzyme bags

Budding yeast cells were streaked on SD-(selective auxotrophic marker) plates and incubated for 2 days at 30 °C. A single yeast colony was then transferred to 10 mL SDC solution and cultured for 18 h at 30 °C and 240 RPM. After counting the cell in a Neubauer improved hemocytometer counting chamber, for each activity assay 5 x 10^7 cells (stationary growth phase) were transferred to 1.5 mL Eppendorf tubes, pelleted, and incubated for 1 h in 1 mL of 0.3% Triton X-100 Tris-KCl buffer (200 mM KCl, 100 mM Tris-HCl, pH 7.4) at 30 °C and 240 RPM. Cells were washed three times with 1 mL NH_4HCO_3 buffer (50 mM, pH 7.4) and then resuspended in 200 μL reaction buffer containing diclofenac (100 μM), NADPH regeneration system (100 μM), and NH_4HCO_3 buffer (50 mM, pH 7.4). Afterward, samples were incubated for 24 h at 37 °C and 230 RPM. For LC-MS-MS analysis, samples were centrifuged at maximum speed for 2 min, the supernatant was collected, and the final liquid was stored at −20 °C until it was analyzed.

2.6. Bioluminescence detection

A concentrated CYP reaction mixture (containing a four-fold concentrated substrate and potassium phosphate buffer) was added to the cell pellets after the permeabilization and washing process. CYP reactions were started by adding the two-fold concentrated NADPH regeneration system. Samples were incubated for 3 h at 37 °C and 1000 RPM. After centrifugation at maximum speed for 2 min, the supernatants were transferred to the white microtiter plates and an equal amount of reconstituted luciferin detection reagent was added to each well. Plates were then incubated at room temperature for 20 min and luminescence was recorded on a Magellan infinite 200Pro microplate reader (Tecan; Männedorf, Switzerland). For the luciferin substrates screening, the specific reaction conditions and substrate concentrations were given in the instructions of the manufacturer (Promega). All measurements were done at least three times in triplicates.

2.7. LC-MS-MS analysis

For the analysis of diclofenac and its metabolite, all samples went through the LC/MS system that consisted of a Q Exactive HF Hybrid Quadrupole-Orbitrap mass spectrometer (Thermo Fisher; Waltham, MA, USA) attached to an Ultimate 3000 RSLC nano system equipped with a reverse phase Agilent Zorbex sb-C18 (4.6 × 150 mm) The phase was 100% water (phase A) and 100% Methanol (phase B), and ran at a constant flow of 0.5 mL/min for 35 min. The gradient used was 0–1 min (90% A: 10% B), 2–6 min (30% B), 7–11 min again (50% B), and 12–16 min (70% B), 17–21 min (90% B), 21–26 (90% B), 27–35 min (90% B). The MS was operated in negative electrospray ionization mode at a capillary voltage of 3800 V. An auxiliary gas flow rate of 12 (arbitrary units) and a sheath gas flow rate of 45 (arbitrary units) with a capillary temperature of 250 °C were used. The final concentration of diclofenac was 100 μM and an injection volume of 20 μL was used.

2.8. Statistical analysis

Data from each experiment was obtained in three replicas. A comparison of the mean value of features (e.g., fluorescence) associated with the engineered strains and controls was carried out using two-sided Welch's *t*-test via IBM SPSS Statistics 26.0, whereas graphs were drawn with GraphPad Prism 6.

3. Results and discussion

The enzymatic Boolean gates that we implemented in *S. cerevisiae* are based on the action of the system CPR-CYP2C9 (from human cells) on different substrates. CPR-CYP2C9 metabolizes the substrate into a product that always represents the gate output. Input are chemicals that modulate the activity of CPR-CYP2C9. A genetic-enzymatic logic gate demands the control of the expression—either at the transcription or translation level—of at least one between CPR and CYP2C9. In our circuits, we used the inducible *GAL1* promoter to trigger the production of CYP2C9 in the presence of galactose. Overall, we managed to build a small collection of basic Boolean gates just by integrating two plasmids for the synthesis of the human CPR and CYP2C9 in the genome of *S. cerevisiae* cells (see Fig. S1).

3.1. Establishing S. cerevisiae enzyme-bag system and its validation on Luc-2FBE and diclofenac substrate

After engineering *S. cerevisiae* strains to behave as enzymatic or genetic-enzymatic logic circuits, we extended to the budding yeast the permeabilized enzyme-bag cell system that was previously developed in *S. pombe* [19] (see Fig. 1). The strain byMM1961, which expresses both CPR and CYP2C9, was treated as described in "Biotransformation with enzyme bags" (see Materials and Methods). However, permeabilization was carried out with different concentrations of Triton X-100 (0–0.3%) in Tris-KCl buffer.

Relative bioluminescence values were measured in triplicates for every Triton X-100 percentage. Our results showed that bioluminescence values gradually increased with ascending concentrations of Triton X-100 (see Fig. 2A). A second evaluation was carried out by using diclofenac as a CYP2C9 substrate. Also in this case, the intensity of 4′-hydroxydilofenac metabolic product gradually increased with growing Triton X-100 percentages (see Fig. 2B).

3.2. Assessing CPR and CYP2C9 expression via fluorescence measurements

In order to avoid false positives and evaluate if the plasmids carrying the human CYP2C9 or its redox partner (CPR) had been integrated in a single or multiple copies, we combined the expression of each of these two proteins with that of the yeast enhanced green fluorescent protein (yEGFP) by using 2A peptide sequences. More precisely, both CYP2C9 and CPR were placed in the first position of a bi-cistronic cassette upstream of the EBRV-1 2A peptide sequence and yEGFP. EBRV-1 was previously reported to have a high cleavage efficiency in eukaryotic cells [21]. The two bi-cistronic sequences were flanked, initially, by the strong yeast constitutive *GPD* promoter (pGPD) and the *CYC1* terminator (CYC1t). They were assembled into integrative *S. cerevisiae-E. coli* shuttle vectors from the pRSII40X collection [29] (see Figs. S2–S3). By measuring green fluorescence via FACS experiments, we determined if the plasmid integration had been successful and how many copies of CPR (first integration) and CYP2C9 (second integration) were expressed.

The first TU (pGPD-CPR-EBRV-1-yEGFP-CYC1t) was integrated in the *URA3* marker. We selected two strains: byMM1959 (the TU was double-integrated) and byMM1960 (single integration). These two strains showed a statistically significant difference between their fluorescence levels (and in comparison, with the negative control strain byMM584—the bare chassis). The second TU (pGPD-CYP2C9-EBRV-1-yEGFP-CYC1t) was integrated only into byMM1959, which resulted in the formation of a third strain (byMM1961) that carried 3 TUs overall, with three copies of *yEGFP*, two of *CPR*, and one of *CYP2C9* (see Fig. 2C). byMM1961 hosts a fully enzymatic circuit that mimics a NOT gate (in the presence of the CORM-401 inhibitor of CYP2C9).

In order to build genetic-enzymatic logic circuits responding to two inputs, we first constructed a new integrative plasmid where the human CYP2C9 and the yEGFP were placed downstream of the galactose-inducible *GAL1* promoter. The new plasmid (carrying pGAL1-CYP2C9-EBRV-1-yEGFP-CYC1t, see Fig. S4) was integrated into byMM1959, which gave rise to the strain byMM2017. Like byMM1961, three copies of *yEGFP* are present inside the genome of byMM2017. In the presence of glucose, pGAL1 is inactive and the fluorescence level from byMM2017 is expected to be close to that corresponding to byMM1959. When

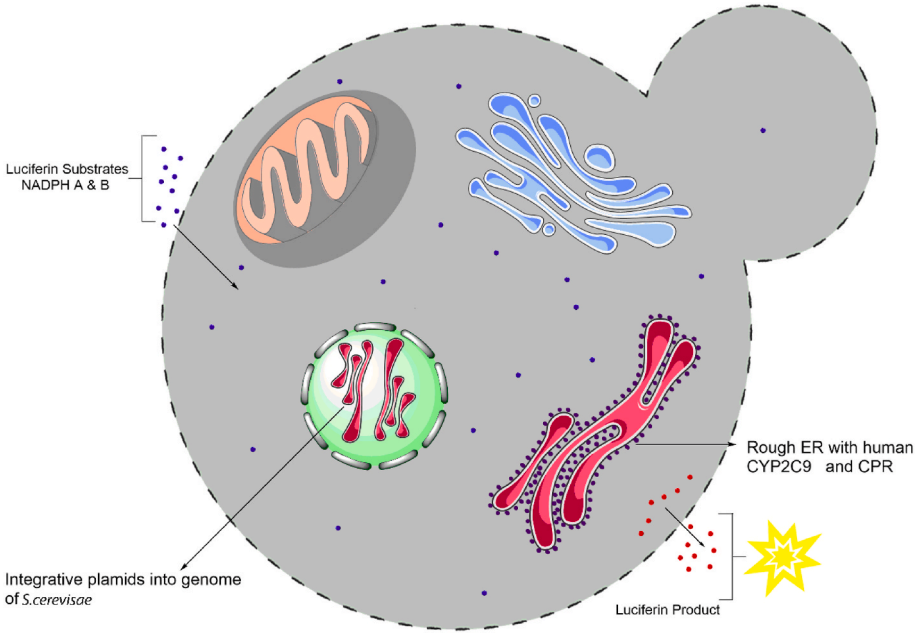

Fig. 1. Schematic representation of recombinant expression of human CRP and CYP2C9 in *S. cerevisiae* together with the enzyme bag-catalyzed biotransformation of luminogenic substrates by the same human CPR-CYP2C9 system. The enzyme-bag method makes use of permeabilized buddying yeast cells that were exposed to Triton X-100.

byMM2017 is cultured in SDC medium supplied with 2% galactose, all three copies of *yEGFP* are transcribed to reach a final fluorescence level that shall not be far from that of byMM1961(see Fig. 2C).

3.3. Functional characterization of *S. cerevisiae* enzyme bags on ten luciferin substrates and diclofenac

We tested the activity of the human CYP2C9 on ten different luciferin substrates (see Table S4). Except for Luc-H (from Promega), these substrates were previously synthesized in-house (and used in *S. pombe* enzyme bags containing various human P450s) [17,26,27]. *S. cerevisiae* strain byMM1961—and its control byMM1959 (expressing only human CPR)—were employed to analyze the biotransformation of the above-mentioned luciferin substrates. In most of these substrates, luciferin is modified by a moiety that is attached to the 6′-carbon via an ether linkage [33]. Upon *O*-dealkylation, the 6′-hydroxy group is freed, and the product can react with luciferase. In addition, certain luciferins contain carboxyl esters instead of a carboxylic acid functional group. In this case, after 6′-hydroxylation or *O*-dealkylation, a further de-esterification step is required to generate luciferin. Finally, aromatic hydroxylation of a luciferin by a CYP enzyme can also provide the 6′-hydroxy group to a substrate that lacks it (as in the case of Luc-H). In the biotransformation of all luciferin substrates, we followed a procedure similar to that adopted in fission yeast [28]. We maintained pH 7.4 throughout all steps (permeabilization, washing, and incubation) of the biotransformation (fission yeast required pH 7.8). Moreover, the incubation time was set to 18 h (as compared to 36 h with fission yeast).

Strain byMM1961 showed significant activities against six substrates as compared to the control group (see Fig. 3). The highest activity of CYP2C9 was observed with Luc-2FBE. A remarkable activity was detected also against Luc-3FBE and Luc-BE (from which both Luc-2FBE and Luc-3FBE are derived [34]). A lower (but statistically significant) activity was associated with Luc-CEE and Luc-FEE. The presence of a chlorine group in luciferin CEE and a fluorine one in luciferin FEE might cause various interactions that involve the active site of the human CYP2C9, which could explain the activities that we have measured. It should also be noted that the activity of the human CYP2C9 against luciferin CEE in *S. cerevisiae* was close to that reported by Promega [35], whereas no activity was found in *S. pombe* [27,35,36]. Finally, we observed also a rather high activity against Luc-H, although much lower than that previously reported in *S. pombe* cells [36,37] (see Fig. S6).

Non-null bioluminescence values detected on the control strain can be attributed to the interaction of the human (and endogenous) CPR with *S. cerevisiae* P450s. Currently, there are five known functional CYP families in budding yeasts, whereas additional six CYP groups—referred to as "orphan CYPs" since their functions were not identified yet—have been documented [38]. CYP51 and CYP61 are involved in the biosynthesis of ergosterol, a fundamental component of the fungal cell membrane [39]. CYP56 [40–42], which catalyzes the reaction to join two *N*-formyl tyrosine molecules to establish an *N*,*N*′-bisformyl dityrosine, is a component of the outer spore wall layer of *S. cerevisiae*. Various P450s, which have not been characterized so far, are also present in phylum Ascomycota (to which *S. cerevisae* belongs) [43]. Strain byMM1959 showed different bioluminescence values towards each different proluciferin substrate, which indicates a potential substrate specificity towards endogenous P450s. Other possible factors that can play a role in the metabolism of proluciferins and xenobiotics in *S. cerevisae* are endogenous enzymes, post translation modifications, and coupling efficiency of CPRs [44].

Human CYP2C9 catalyzes the metabolism of diclofenac to 4′-hydroxydiclofenac [45,46] (see Fig. S7). The LC-MS-MS analysis on byMM1961 (constitutive expression of human CYP2C9) showed 4′-hydroxydiclofenac at a retention time of 17.37 min. The mass peak (LC-QE-MS, $[M-H]^-$) of the 4′-hydroxydiclofenac product [46,47] ($C_{14}H_{11}Cl_2NO_3$) from the permeabilized *S. cerevisiae* cells corresponded to $[M-H]^- = 310.0028$ Da (see Figs. S8–S9). The negative control byMM1959 did not show any product peak. The corresponding extracted ion chromatogram (LC-QE-MS, $[M-H]^-$) and full mass scan are shown in Figs. S10–S11. Moreover, the diclofenac (substrate) peak (LC-QE-MS, $[M-H]^-$) eluted out at 23.33 min [48–50] and extracted ion chromatogram (LC-QE-MS, $[M-H]^-$) of diclofenac [51–53] are shown in Figs. S12–S13.

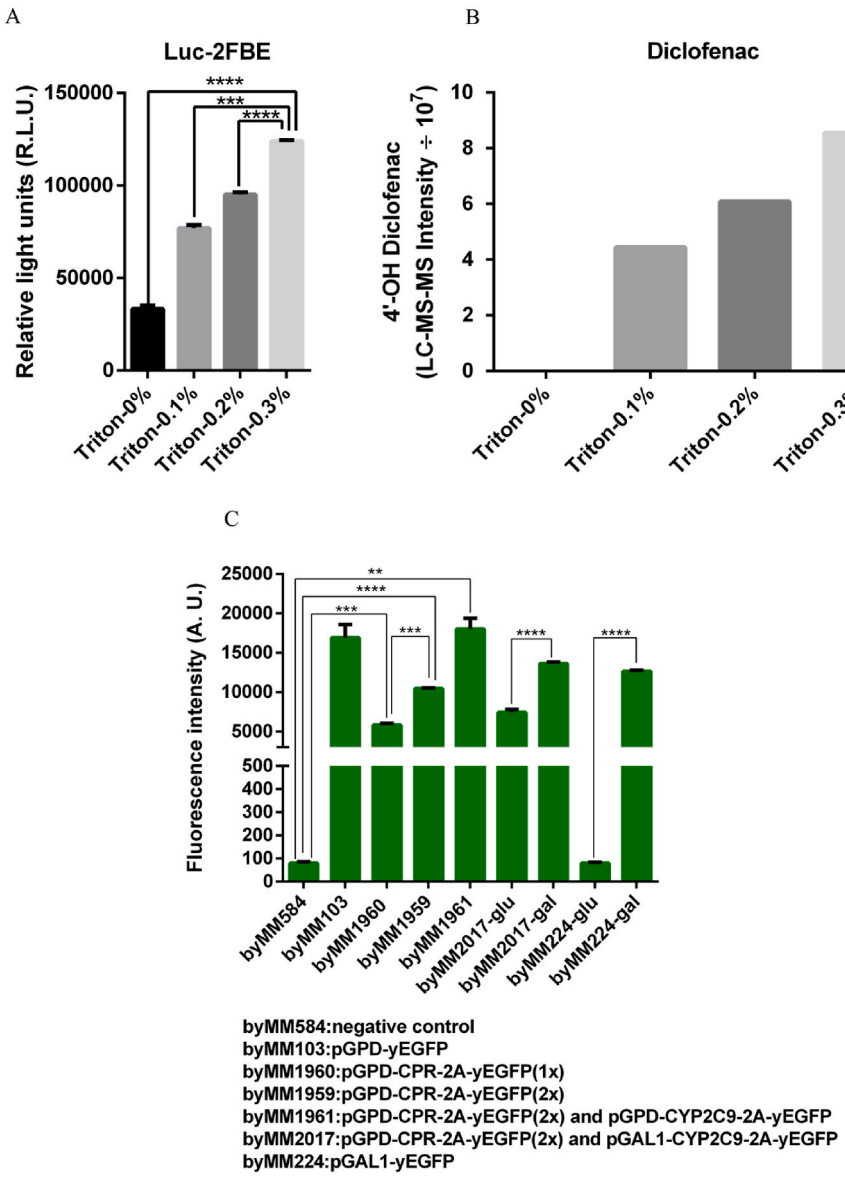

Fig. 2. Enzyme bags and fluorescence expression in S. cerevisiae. (**A-B**) Validation of the enzyme-bag system in *S. cerevisiae*. Strain byMM1961 was permeabilized with increasing concentrations of Triton X-100. (A) Relative light units (R.L.U.) and (B) 4′-hydroxydilofenac intensity as a function of Triton X-100 solution percentage. Both signals grew by increasing the amount of Triton X-100 in the cell permeabilization process. The two substrates luciferin 2FBE and diclofenac were used at a concentration of 150 μM and 100 μM, respectively. Bioluminescence was measured in three independent experiments. The non-zero bioluminescence signal in the absence of Triton X-100 is caused by a partial permeabilization of byMM1961 since Luc-2FBE was dissolved in DMSO (see Fig. S5). The product 4′-hydroxydiclofenac was not detected without Triton X-100. (**C**) Fluorescence expressed by yeast strains engineered with bicistronic sequences and their controls. The fluorescence reached by byMM1959 is about 1.80-fold higher than that corresponding to byMM1960, which indicates that a double integration of the TU carrying CPR has taken place. The positive control byMM103 (pGPD-yEGFP-CYC1t) returns roughly as much fluorescence as byMM1961, whose genome contains three copies of *yEGFP*. Compared to byMM1960, byMM103 fluorescence is 2.91-fold higher. Therefore, the presence of the ERBV-1 2A peptide sequence reduces by ~2/3 the fluorescence driven by pGPD. In the presence of galactose, byMM2017 fluorescence level becomes 1.83-fold higher than that in the presence of glucose, which confirms that the new integrative plasmid has been inserted into the yeast genome. CYCP2C9 activity is expected to resemble byMM224 fluorescence-expression pattern: very high upon induction with galactose and negligible in glucose-containing media (** p-value <0.01; *** p-value <0.001; **** p-value <0.0001; two-sided Welch's *t*-test). Fluorescence intensity is expressed in arbitrary units (A. U.).

3.4. Use of a CORM (CO-releasing molecule) for inhibiting human CYP2C9 activity. Construction of enzymatic NOT gates

CO-releasing molecules (CORMs) such as CORM-401 are of considerable interest for basic research and drug development [54,55]. CO from CORM-401 is recognized as a signaling molecule in various cellular processes [56,57] and CORM-401 has previously been used as an inhibitor of CYP1A2 [22,58]. Regulation of CYP-dependent metabolism of xenobiotics via repression of CYPs by CORM-401 has been examined too [22].

CORM-401 is a chelating compound in which a variable number of CO molecules are trapped inside. It is used to deliver carbon monoxide directly and at low concentrations at target sites [22]. In our experimental setting, these CO molecules can bind to the Fe^{+2} in the heme of CYP2C9 (see Fig. S14), thereby inactivating it. We have tested CORM-401 against two luciferin substrates (Luc-2FBE and Luc-3FBE) and diclofenac to realize three enzymatic NOT gates based on the strain byMM1961. A NOT gate takes a single binary input and returns "0" as an output when the input is equal to "1", and "1" when the input is "0" (see Fig. 4A). To check the functionality of the NOT gates, strain

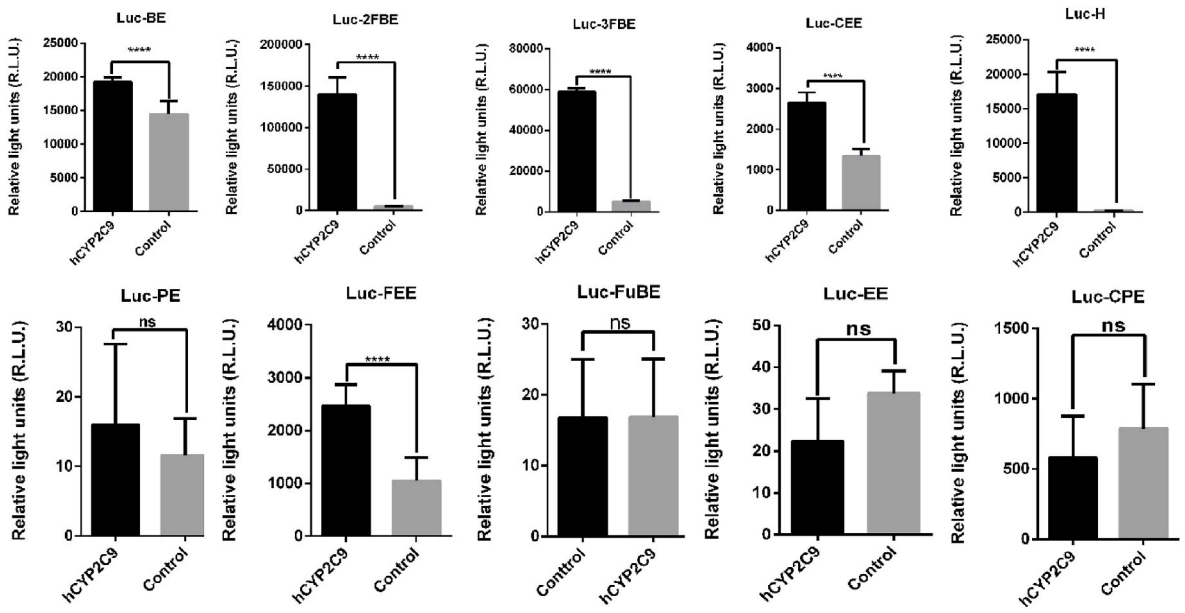

Fig. 3. Activity of the human CYP2C9 (hCYP2C9) on ten luminogenic substrates via *S. cerevisiae* enzyme bags. For each measurement, 150 μM of luminogenic substrate (only 100 μM of Luc-H) were used. byMM1959 was checked in parallel as a control strain. Mean activity levels, calculated on at least three independent experiments, are expressed in relative light units—R.L.U. (***: p-value <0.001; ****: p-value <0.0001; ns: no significant difference; two-sided Welch's *t*-test).

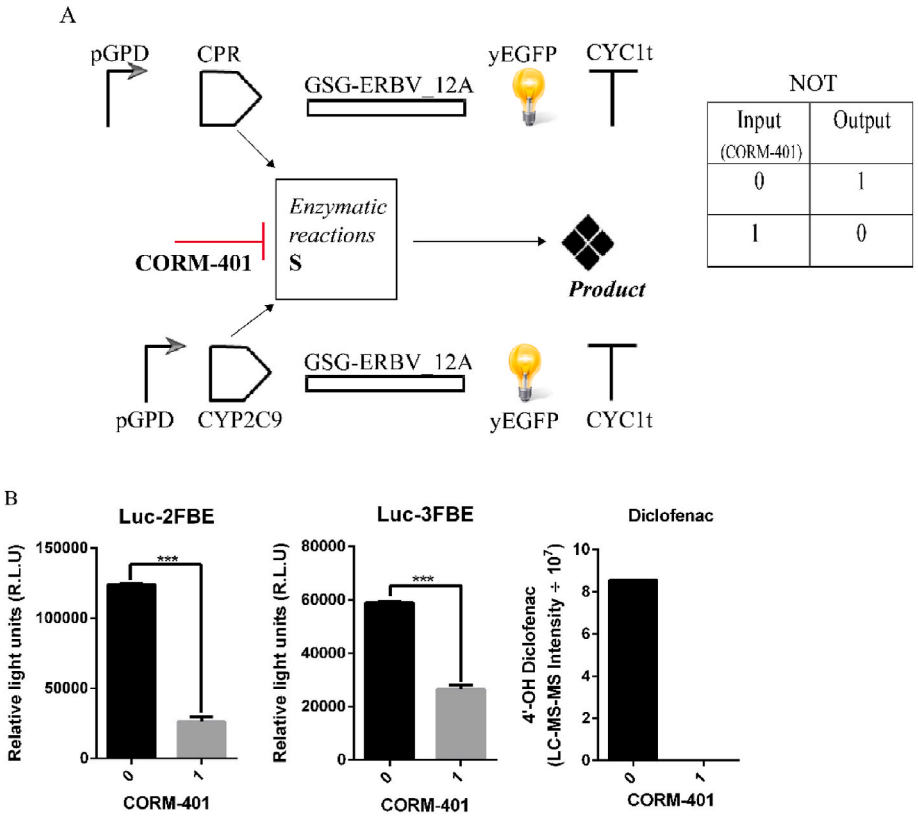

Fig. 4. Enzymatic NOT gates based on the CPR-CYP2C9 system. (**A**) In the presence of a substrate **S**—here represented inside an enzymatic reaction pool [60]—CPR-CYP2C9 catalizes the synthesis of a product that corresponds to the output signal of the gate. The only input is CORM-401 (200 μM in the presence of Luc-2FBE and Luc-3FBE, 500 μM in the presence of diclofenac). Black arrows indicate fluxes of (macro-)molecules towards and from the enzymatic reaction pool. The red hammer-like line means inhibition of CYP2C9 activity. (**B**) NOT gate performance (***: p-value <0.001; two-sided Welch's *t*-test). We also checked the inhibitory action of CORM-401 on byMM1959 that returned a moderate bioluminescence in the presence of the two luciferin substrates. Results are shown in Fig. S16.

byMM1961 was grown in SDC media for 18 h. Biotransformations of three substrates (Luc-2FBE, Luc-3FBE, and diclofenac) were performed as described above. Our results show that the three NOT gates performed correctly, as bioluminescence values corresponding to the absence of CORM-401 (input = 0) were statistically significantly higher than those detected in the presence of CORM-401 (input = 1). Moreover, the

ON/OFF ratio (i.e., the quotient between "1" and "0" output values) reached 4.78 for Luc-2FBE, 2.23 for Luc-3FBE (both above the working threshold of 2 [59]) and infinite for diclofenac (see Fig. 4B). Indeed, 500 μM CORM-401 completely repressed CYP2C9-CPR activity on 100 μM diclofenac (see Fig. S15).

3.5. A genetic-enzymatic YES Boolean gate sensing galactose

YES (or buffer) gates are devices that produce a logic output identical to the only input they take. A common way to implement genetic YES gates requires exploiting the interaction between repressor proteins and their corresponding inducers. For instance, the DNA-binding state of TetR and LacI can be changed by tetracycline and IPTG, respectively. In the absence of their inducers (the gate input), these two repressors bind their operator(s) placed between the TATA box and the TSS (transcription start site) of a synthetic promoter and repress fluorescence expression, i.e., the gate output is 0. In contrast, upon forming a complex with the corresponding input chemical, both TetR and LacI are no longer able to bind the DNA. Hence, a fluorescence signal is produced, i.e., the output is 1[21].

In this study, we have established a novel genetic-enzymatic YES gate by expressing the human CYP2C9 under the inducible promoter pGAL1, i.e., a genetic switch. The circuit output, bioluminescence, is due to the enzymatic interaction between CYP2C9 and a luciferin substrate (see Fig. 5A). In order to maximize the gate performance and have a "0" output signal as low as possible, we considered, as substrates for our gate, the three ones that showed the smallest activity with byMM1959, i.e., in the absence of the human CYP2C9. These were Luc-H, Luc-FEE, and Luc-CEE (see Fig. 3). Initially, we selected Luc-H and varied its concentration to find a value that could guarantee a high output signal when CYP2C9 expression was driven by pGAL1 (strain byMM2017). From the titration curve in Fig. 5B, we selected 100 μM as the substrate concentration. Afterward, we measured bioluminescence in the presence and absence of this amount of the selected luminogenic substrates. Luc-H led to the most performant YES gate, whose ON/OFF ratio corresponded to 76.98 (see Fig. 5C).

We further built a YES gate that used diclofenac (100 μM) as a substrate (see Fig. 5D). The LC-MS-MS analysis on byMM2017 grown in SDC supplied with 2% galactose showed that 4′ hydroxydiclofenac product at a retention time of 16.58 min. The mass peak (LC-QE-MS, $[M-H]^-$) of the 4′-hydroxydiclofenac product [46,47] ($C_{14}H_{11}Cl_2NO_3$), obtained via enzyme bags, corresponded to $[M-H]^- = 310.0032$ Da (see Ta ble 1 and Figs. S17–S18). The negative control, i.e., byMM2017 cultured in SDC supplemented with 2% glucose did not show any product peak (see Figs. S19 and S20).

3.6. A genetic-enzymatic N-IMPLY gate

We build a two-input genetic-enzymatic N-IMPLY gate by merging the YES and NOT gates described above. In other words, we combined the galactose-inducible synthesis of the human CYP2C9 with the inhibitory action of CORM-401 on the activity of the enzyme on the Luc-H substrate (see Fig. 6A). First, we determined, with a titration curve, that 400 μM CORM-401 could completely repress CYP2C9 activity on 100 μM Luc-H—the yeast strain hosting the circuit was byMM2017 (see Fig. 6B). Then, we measured the bioluminescence values for the two entries of the truth table characterized by the absence of galactose. The four output values in Fig. 6C represented faithfully the gate truth table and let us to evaluate the gate performance in term of the ρ-value [9], here corresponding to the ratio between the only one "1" output and the highest of the three "0" outputs, i.e., the fluorescence intensities associated with the "10" and "00" truth table entry, respectively. Since both

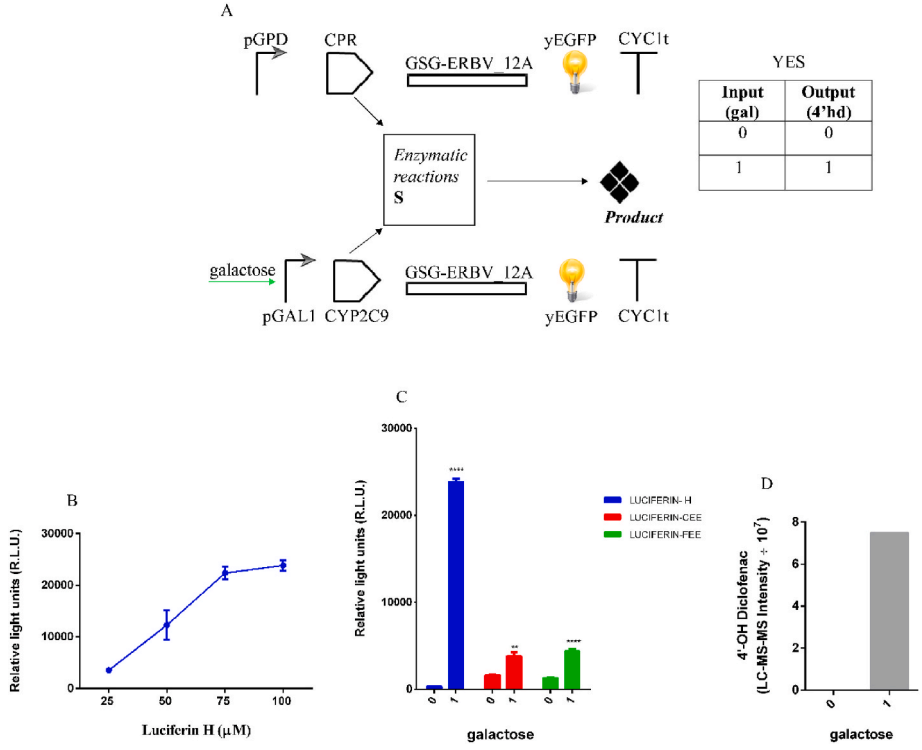

Fig. 5. Genetic-enzymatic galactose-sensing YES gate. **(A)** Circuit scheme. Only in the presence of galactose, CYP2C9 is expressed and activated by CPR. CYP2C9 activity on a luciferin substrate produces the output signal (bioluminescence). The green arrow represents activation of transcription from the *GAL1* promoter. **(B)** Growing bioluminescence was detected from strain byMM2017 for increasing concentrations of Luc-H. **(C)** YES gate performance by varying the luminogenic substrate. The activity of CYP2C9—on 100 μM of the three luciferin substrates that minimized the background activity from strain byMM1959—is reported in the presence and absence of galactose. The ON/OFF ratio in the presence of Luc-CEE is 2.33, whereas it reaches 3.68 with Luc-FEE. **(D)** YES gate performance on diclofenac (**: p_value < 0.01; ****: p-value <0.0001; two-sided Welch's *t*-test).

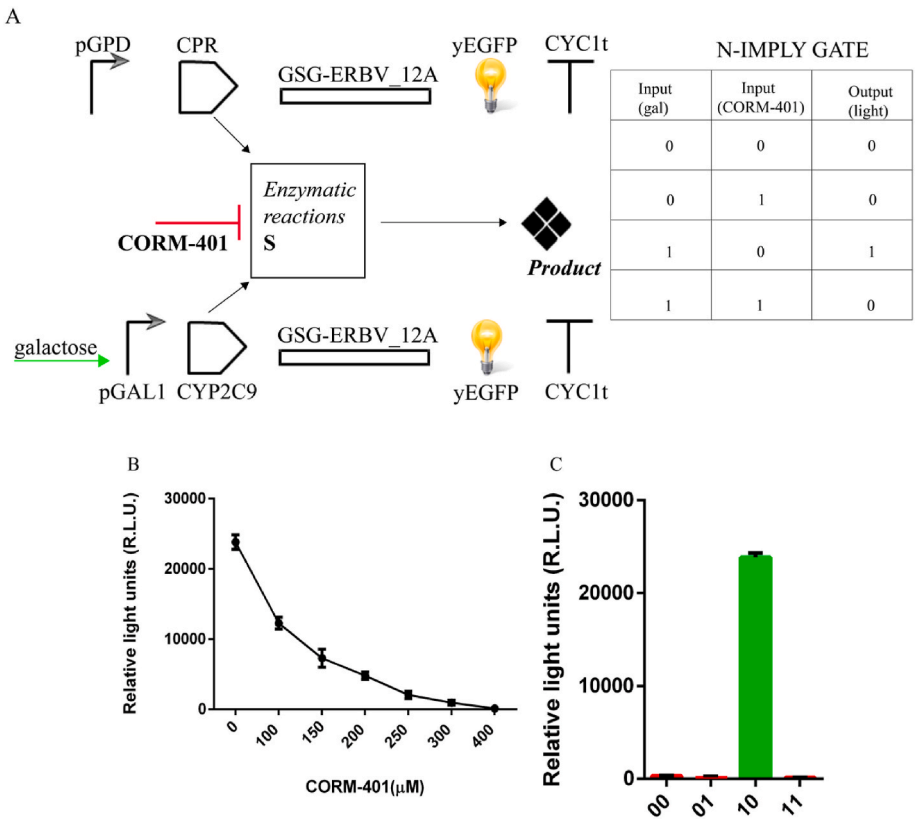

Fig. 6. Genetic-enzymatic N-IMPLY gate sensing galactose and CORM-401. **(A)** Circuit scheme. The sole "1" output is achieved by the simultaneous presence of galactose and absence of CORM-401. **(B)** Bioluminescence decreases with increasing concentration of CORM-401. byMM2017 was grown in SDC medium supplied with 2% galactose. Luc-H (100 μM) was chosen as a substrate for CYP2C9 activity. **(C)** Performance of the N-IMPLY gate.

fluorescence levels were detected in the absence of CORM-401, the N-IMPLY ρ-value turned out to be identical to the ON/OFF ratio of the YES gate using Luc-H as a substrate, namely: 76.98.

4. Conclusion

Synthetic biology has led to the engineering of genetic/enzymatic tools to reprogram microorganisms for the enhanced expression of heterogeneous drug metabolic enzymes. Significant progress has been made in the creation of chassis organisms, biological circuits, and high-throughput screening technologies that helped accelerate the current drug discovery cycle. *S. cerevisiae,* as a chassis, has played a crucial role due to its robust applicability, cellular reprogrammability, and excellent characterization.

Here, we have shown a novel way to engineer (genetic)-enzymatic Boolean gates in *S. cerevisiae* based on the human CYP2C9 and its redox partner CPR. Yeast cells, first, drive the expression of CYP2C9 and CPR. Then, cells are permeabilized as enzyme bags such that CYP2C9 can interact with a substrate (luciferin substrate or diclofenac) and release a product (bioluminescence or a diclofenac metabolite) that is finally measured with a proper machine. Furthermore, enzyme bags allow controlling CYP2C9 via the CORM-401 inhibitor, whereas the production of CYP2C9 was regulated during the cell-growth, by placing the *CYP2C9* gene under the galactose-inducible *GAL1* promoter.

In general, our new Boolean gates showed high performance, especially when CORM-401 was used as an input, due to its extremely strong action on CYP2C9. Moreover, logic circuits in *S. cerevisiae* will be applied to drug development. Yeasts that have been engineered as Boolean gates respond to specific inputs by releasing a fluorescence/luminescence signal. This kind of outputs will help the screening for drugs responsible of various cellular responses.

Logic gates together with an optimized *S. cerevisiae* chassis can facilitate comparative studies on both human P450s metabolism and the effects due to their variants. To this aim, we shall expedite the drug development processes and identify novel active potential compounds.

Funding

No funding.

Data availability

FACS data are available at: http://flowrepository.org/id/RvFrKC97NV4hdI9Dk8ZFRUQRMDvubP1Epn6DQgdcyrRh9v5s23LAgqQB5qiXnvVa.

CRediT authorship contribution statement

Rana Azeem Ashraf: making experiments, Formal analysis, Writing – original draft. **Matthias Bureik:** Conceptualization, Writing – review & editing. **Mario Andrea Marchisio:** Conceptualization, Supervision, Writing – review & editing.

Declaration of competing interest

The authors declare that they have no known competing financial interests or personal relationships that could have appeared to influence the work reported in this paper.

Acknowledgements

We sincerely thank all students of the Synthetic Biology Laboratory at the School of Pharmaceutical Science and Technology—Tianjin University for their kind help. We want to express our gratitude to Zhi Li and

Xiangyang Zhang for their assistance in FACS experiments and Gao Yan for her assistance in LC-MS-MS analysis.

Appendix A. Supplementary data

Supplementary data to this article can be found online at https://doi.org/10.1016/j.synbio.2024.03.013.

References

[1] Tugendreich S, Bassett Jr DE, McKusick VA, Boguski MS, Hieter P. Genes conserved in yeast and humans. From NLM Hum Mol Genet 1994;3(Spec No):1509–17. https://doi.org/10.1093/hmg/3.suppl_1.1509.

[2] van Leeuwen J, Vermeulen NPE, Chris Vos J. Yeast as a humanized model organism for biotransformation-related toxicity. Curr Drug Metabol 2012;13 10:1464–75.

[3] Truong DM, Boeke JD. Resetting the yeast epigenome with human nucleosomes. From NLM Cell 2017;171(7):1508–1519.e1513. https://doi.org/10.1016/j.cell.2017.10.043.

[4] Simon JA, Bedalov A. Yeast as a model system for anticancer drug discovery. Nat Rev Cancer 2004;4(6):481–7. https://doi.org/10.1038/nrc1372.

[5] McDonald MG, Ray S, Amorosi CJ, Sitko KA, Kowalski JP, Paco L, Nath A, Gallis B, Totah RA, Dunham MJ, et al. Expression and functional characterization of breast cancer-associated cytochrome P450 4Z1 in Saccharomyces cerevisiae</em&gt. Drug Metabol Dispos 2017;45(12):1364–71. https://doi.org/10.1124/dmd.117.078188.

[6] Yu L, Marchisio MA. CRISPR-associated type V proteins as a tool for controlling mRNA stability in S. cerevisiae synthetic gene circuits. From NLM Nucleic Acids Res 2023;51(3):1473–87. https://doi.org/10.1093/nar/gkac1270.

[7] Feldmann H. Yeast: molecular and cell biology. 2010.

[8] Benenson Y. Biomolecular computing systems: principles, progress and potential. Nat Rev Genet 2012;13(7):455–68. https://doi.org/10.1038/nrg3197.

[9] Marchisio MA, Stelling J. Automatic design of digital synthetic gene circuits. PLoS Comput Biol 2011;7(2). ARTN e100108310.1371/journal.pcbi.1001083.

[10] Erbas-Cakmak S, Kolemen S, Sedgwick AC, Gunnlaugsson T, James TD, Yoon J, Akkaya EU. Molecular logic gates: the past, present and future. Chem Soc Rev 2018;47(7):2228–48. https://doi.org/10.1039/c7cs00491e.

[11] Lewin B. Genes IX. Jones and Bartlett Publishers; 2008.

[12] Nebert DW, Wikvall K, Miller WL. Human cytochromes P450 in health and disease. Philos Trans R Soc Lond B Biol Sci 2013;368(1612):20120431. https://doi.org/10.1098/rstb.2012.0431.

[13] Sharma SS, Sharma S, Bureik M. Screening of the whole human cytochrome P450 complement (CYPome) with enzyme bag cocktails. J Pharm Anal 2020;10(3):271–6. https://doi.org/10.1016/j.jpha.2020.05.003.

[14] Alberts B. Model organisms and human health. Science 2010;330(6012). https://doi.org/10.1126/science.1201826. 1724-1724.

[15] Sharma S, Sharma SS, Zhang X, Bureik JP, Sorensen EJ, Bureik M. Conversion of five proluciferin esters by human cytochrome P450 enzymes. Biotechnol J 2021;16(7). ARTN e210000710.1002/biot.202100007.

[16] Zhao J, Liu SJ, Wolf CA, Wolber G, Parr MK, Bureik M. Changes in alprazolam metabolism by CYP3A43 mutants. Biomedicines 2022;10(12). DOI: ARTN 302210.3390/biomedicines10123022.

[17] Liu JY, Machalz D, Wolber G, Sorensen EJ, Bureik M. New proluciferin substrates for human CYP4 family enzymes. Appl Biochem Biotechnol 2021;193(1):218–37. https://doi.org/10.1007/s12010-020-03388-6.

[18] Weldemichael DM, Zhou K, Su SJ, Zhao L, Marchisio MA, Bureik M. Futile cycling by human microsomal cytochrome P450 enzymes within intact fission yeast cells. Arch Biochem Biophys 2021;701. ARTN 10879110.1016/j.abb.2021.108791.

[19] Yan Q, Machalz D, Zollner A, Sorensen EJ, Wolber G, Bureik M. Efficient substrate screening and inhibitor testing of human CYP4Z1 using permeabilized recombinant fission yeast. Biochem Pharmacol 2017;146:174–87. https://doi.org/10.1016/j.bcp.2017.09.011.

[20] Souza-Moreira TM, Navarrete C, Chen X, Zanelli CF, Valentini SR, Furlan M, Nielsen J, Krivoruchko A. Screening of 2A peptides for polycistronic gene expression in yeast. From NLM FEMS Yeast Res 2018;18(5). https://doi.org/10.1093/femsyr/foy036.

[21] Wang X, Tian X, Marchisio MA. Logic circuits based on 2A peptide sequences in the yeast Saccharomyces cerevisiae. ACS Synth Biol 2023;12(1):224–37. https://doi.org/10.1021/acssynbio.2c00506.

[22] Walter M, Stahl W, Brenneisen P, Reichert AS, Stucki D. Carbon monoxide releasing molecule 401 (CORM-401) modulates phase I metabolism of xenobiotics. Toxicol Vitro 2019;59:215–20. https://doi.org/10.1016/j.tiv.2019.04.018.

[23] Daniel Gietz R, Woods RA. Transformation of yeast by lithium acetate/single-stranded carrier DNA/polyethylene glycol method. In: Guthrie C, Fink GR, editors. Methods in enzymology, 350. Academic Press; 2002. p. 87–96.

[24] Crook SH, Mann BE, Meijer AJHM, Adams H, Sawle P, Scapens D, Motterlini R. [Mn(CO)4{S2CNMe(CH2CO2H)}], a new water-soluble CO-releasing molecule. Dalton Trans 2011;40(16):4230–5. https://doi.org/10.1039/C1DT10125K. 10.1039/C1DT10125K.

[25] Fayad-Kobeissi S, Ratovonantenaina J, Dabiré H, Wilson JL, Rodriguez AM, Berdeaux A, Dubois-Randé J-L, Mann BE, Motterlini R, Foresti R. Vascular and angiogenic activities of CORM-401, an oxidant-sensitive CO-releasing molecule. Biochem Pharmacol 2016;102:64–77. https://doi.org/10.1016/j.bcp.2015.12.014.

[26] Sharma S, Liu J, Zhang X, Sharma SS, Sorensen EJ, Bureik M. New luciferin-based probe substrates for human CYP26A1. Biochemistry and biophysics reports 2020;24:100861.

[27] Zhao J, Zhang X, Wang Y, Huang H, Sharma S, Sharma SS, Wolf CA, Liu S, Wolber G, Sorensen EJ, et al. Exploring the chemical space of proluciferins as probe substrates for human cytochrome P450 enzymes. From NLMMedline Appl Biochem Biotechnol 2023;195(2):1042–58. https://doi.org/10.1007/s12010-022-04184-0.

[28] Sharma S, Durairaj P, Bureik M. Rapid and convenient biotransformation procedure for human drug metabolizing enzymes using permeabilized fission yeast cells. From NLM Anal Biochem 2020;607:113704. https://doi.org/10.1016/j.ab.2020.113704.

[29] Chee MK, Haase SB. New and redesigned pRS plasmid shuttle vectors for genetic manipulation of Saccharomyces cerevisiae (acccessed 1/5/2024) G3 Genes|Genomes|Genetics 2012;2(5):515–26. https://doi.org/10.1534/g3.111.001917.

[30] Gibson DG, Young L, Chuang R-Y, Venter JC, Hutchison CA, Smith HO. Enzymatic assembly of DNA molecules up to several hundred kilobases. Nat Methods 2009;6(5):343–5. https://doi.org/10.1038/nmeth.1318.

[31] F SJ, Russell D. Molecular cloning: a laboratory manual (*3-volume set*). 2001.

[32] Hahne F, LeMeur N, Brinkman RR, Ellis B, Haaland P, Sarkar D, Spidlen J, Strain E, Gentleman R. flowCore: a Bioconductor package for high throughput flow cytometry. BMC Bioinf 2009;10(1):106. https://doi.org/10.1186/1471-2105-10-106.

[33] Cali JJ, Ma D, Wood MG, Meisenheimer PL, Klaubert DH. Bioluminescent assays for ADME evaluation: dialing in CYP selectivity with luminogenic substrates. From NLM Expet Opin Drug Metabol Toxicol 2012;8(9):1115–30. https://doi.org/10.1517/17425255.2012.695345.

[34] Liu J, Machalz D, Wolber G, Sorensen EJ, Bureik M. New proluciferin substrates for human CYP4 family enzymes. Appl Biochem Biotechnol 2021;193(1):218–37.

[35] Cali JJ, Ma D, Sobol M, Simpson DJ, Frackman S, Good TD, Daily WJ, Liu D. Luminogenic cytochrome P450 assays. From NLM Expet Opin Drug Metabol Toxicol 2006;2(4):629–45. https://doi.org/10.1517/17425255.2.4.629.

[36] Durairaj P, Fan L, Du W, Ahmad S, Mebrahtu D, Sharma S, Ashraf RA, Liu J, Liu Q, Bureik M. Functional expression and activity screening of all human cytochrome P450 enzymes in fission yeast. From NLM FEBS Lett 2019;593(12):1372–80. https://doi.org/10.1002/1873-3468.13441.

[37] Chang Q, Berdyshev E, Cao D, Bogaard J, White J, Chen S, Shah R, Mu W, Grantner R, Bettis S, et al. Cytochrome P450 2C epoxygenases mediate photochemical stress-induced death of photoreceptors. J Biol Chem 2014;289. https://doi.org/10.1074/jbc.M113.507152.

[38] Linder T. Taxonomic distribution of cytochrome P450 monooxygenases (CYPs) among the budding yeasts (Sub-Phylum saccharomycotina). From NLM Microorganisms 2019;7(8). https://doi.org/10.3390/microorganisms7080247.

[39] Kelly SL, Lamb DC, Kelly DE. Sterol 22-desaturase, cytochrome P45061, possesses activity in xenobiotic metabolism. From NLM FEBS Lett 1997;412(1):233–5. https://doi.org/10.1016/s0014-5793(97)00785-0.

[40] Briza P, Eckerstorfer M, Breitenbach M. The sporulation-specific enzymes encoded by the DIT1 and DIT2 genes catalyze a two-step reaction leading to a soluble LL-dityrosine-containing precursor of the yeast spore wall. Proc Natl Acad Sci USA 1994;91(10):4524–8.

[41] Briza P, Kalchhauser H, Pittenauer E, Allmaier G, Breitenbach MN. N'-Bisformyl dityrosine is an in vivo precursor of the yeast ascospore wall. From NLM Eur J Biochem 1996;239(1):124–31. https://doi.org/10.1111/j.1432-1033.1996.0124u.x.

[42] Melo NR, Moran GP, Warrilow AG, Dudley E, Smith SN, Sullivan DJ, Lamb DC, Kelly DE, Coleman DC, Kelly SL. CYP56 (Dit2p) in Candida albicans: characterization and investigation of its role in growth and antifungal drug susceptibility. From NLM Antimicrob Agents Chemother 2008;52(10):3718–24. https://doi.org/10.1128/aac.00446-08.

[43] Chen W, Lee M-K, Jefcoate C, Kim S-C, Chen F, Yu J-H. Fungal cytochrome P450 monooxygenases: their distribution, structure, functions, family expansion, and evolutionary origin. acccessed 12/10/2023 Genome Biology and Evolution 2014;6(7):1620–34. https://doi.org/10.1093/gbe/evu132.

[44] Duan H, Schuler MA. Heterologous expression and strategies for encapsulation of membrane-localized plant P450s. Phytochemistry Rev 2006;5:507–23.

[45] Mancy A, Antignac M, Minoletti C, Dijols S, Mouries V, Duong NT, Battioni P, Dansette PM, Mansuy D. Diclofenac and its derivatives as tools for studying human cytochromes P450 active sites: particular efficiency and regioselectivity of P450 2Cs. From NLM Biochemistry 1999;38(43):14264–70. https://doi.org/10.1021/bi991195u.

[46] Leemann T, Transon C, Dayer P. Cytochrome P450TB (CYP2C): a major monooxygenase catalyzing diclofenac 4'-hydroxylation in human liver. From NLM Life Sci 1993;52(1):29–34. https://doi.org/10.1016/0024-3205(93)90285-b.

[47] Drăgan CA, Peters FT, Bour P, Schwaninger AE, Schaan SM, Neunzig I, Widjaja M, Zapp J, Kraemer T, Maurer HH, et al. Convenient gram-scale metabolite synthesis by engineered fission yeast strains expressing functional human P450 systems. From NLM Appl Biochem Biotechnol 2011;163(8):965–80. https://doi.org/10.1007/s12010-010-9100-3.

[48] Sarda S, Page C, Pickup K, Schulz-Utermoehl T, Wilson I. Diclofenac metabolism in the mouse: novel in vivo metabolites identified by high performance liquid chromatography coupled to linear ion trap mass spectrometry. From NLM Xenobiotica; the fate of foreign compounds in biological systems 2012;42(2):179–94. https://doi.org/10.3109/00498254.2011.607865.

[49] Kosjek T, Žigon D, Kralj B, Heath E. The use of quadrupole-time-of-flight mass spectrometer for the elucidation of diclofenac biotransformation products in wastewater. J Chromatogr A 2008;1215(1):57–63. https://doi.org/10.1016/j.chroma.2008.10.111.

[50] Kosjek T, Zigon D, Kralj B, Heath E. The use of quadrupole-time-of-flight mass spectrometer for the elucidation of diclofenac biotransformation products in wastewater. From NLM J Chromatogr A 2008;1215(1–2):57–63. https://doi.org/10.1016/j.chroma.2008.10.111.

[51] Tateishi Y, Ohe T, Ogawa M, Takahashi K, Nakamura S, Mashino T. Development of novel diclofenac analogs designed to avoid metabolic activation and hepatocyte toxicity. From NLM ACS Omega 2020;5(50):32608–16. https://doi.org/10.1021/acsomega.0c04942.

[52] Ngui JS, Tang W, Stearns RA, Shou M, Miller RR, Zhang Y, Lin JH, Baillie TA. Cytochrome P450 3A4-mediated interaction of diclofenac and quinidine. Drug Metabol Dispos 2000;28(9):1043–50.

[53] Sarkar U, Ravindra KC, Large E, Young CL, Rivera-Burgos D, Yu J, Cirit M, Hughes DJ, Wishnok JS, Lauffenburger DA, et al. Integrated assessment of diclofenac biotransformation, pharmacokinetics, and omics-based toxicity in a three-dimensional human liver-immunocompetent coculture system. From NLM Drug Metabol Dispos: the biological fate of chemicals 2017;45(7):855–66. https://doi.org/10.1124/dmd.116.074005.

[54] Hopper CP, Meinel L, Steiger C, Otterbein LE. Where is the clinical breakthrough of heme oxygenase-1/carbon monoxide therapeutics?. From NLM Curr Pharmaceut Des 2018;24(20):2264–82. https://doi.org/10.2174/1381612824666180723161811.

[55] Motterlini R, Foresti R. Biological signaling by carbon monoxide and carbon monoxide-releasing molecules. From NLM Am J Physiol Cell Physiol 2017;312(3):C302–c313. https://doi.org/10.1152/ajpcell.00360.2016.

[56] Stucki D, Krahl H, Walter M, Steinhausen J, Hommel K, Brenneisen P, Stahl W. Effects of frequently applied carbon monoxide releasing molecules (CORMs) in typical CO-sensitive model systems - a comparative in vitro study. From NLM Arch Biochem Biophys 2020;687:108383. https://doi.org/10.1016/j.abb.2020.108383.

[57] Khan H, Faizan M, Niazi SUK, Madiha, Muhammad N, Zhang W. Water-Soluble carbon monoxide-releasing molecules (CORMs). From NLM Top Curr Chem 2022;381(1):3. https://doi.org/10.1007/s41061-022-00413-6.

[58] Leemann T, Bonnabry P, Dayer P. Selective inhibition of major drug metabolizing cytochrome P450 isozymes in human liver microsomes by carbon monoxide. X Scopus Life Sci 1994;54(14):951–6. https://doi.org/10.1016/0024-3205(94)00496. Article.

[59] Abraha BW, Marchisio MA. NOT gates based on protein degradation as a case study for a new modular modeling via SBML level 3-comp package. From NLM Front Bioeng Biotechnol 2022;10:845240. https://doi.org/10.3389/fbioe.2022.845240.

[60] Marchisio MA, Stelling J. Computational design of synthetic gene circuits with composable parts. From NLM Bioinformatics 2008;24(17):1903–10. https://doi.org/10.1093/bioinformatics/btn330.